Electronic Supplementary Information

Synthesis and Modification of Non-Isocyanate Thermoplastic Polyurethane (TPU) from Recycled Waste Electrolytes

*Xiaolong Li [a], Haiyue Wang [a], Liying Guo *[a], Ruibo Wang [b], Zhijiong Wu [b]*

a: Shenyang University of Technology, Liaoyang, People's Republic of China

b: CNPC Research Institute of Safety and Environment Technology Dalian Department

**Corresponding author: Prof. Liying Guo, E-mail:* lyguo1981@sut.edu.cn

General Information

The supporting information includes fourteen pages, two tables and eleven figures.

Data Availability Summary

This Supplementary Information file contains the following data supporting the findings in the main article:

Figure S1: GC-MS curve (a) HBC composition and proportion; (b) LBC composition and proportion. These data support the experimental procedures described in Section 2.3 and 2.4.

Figure S2: Principle of synthesis of dicarbamate. It provides a theoretical basis for the synthesis of aromatic dicarbamate.

Table S1: GC-MS Characterization Data of High/Low-Boiling Point Components in Waste Electrolyte.

Table S2: Orthogonal experimental design for TPU modification. These data provide corresponding preparation protocols for the various types of TPU mentioned in the article.

Figures S3-S6: Full ^{1}H NMR spectra of all of PES performed polymer. These data

support the characterization results shown in Figures 2.

Figures S7-S10: Full NMR spectra (^{1}H and ^{13}C) of four types of TPU. These data support the characterization results shown in Figures 4.

Figures S11: GPC curve of eight types of TPU. This figure supports the data source of Table 3.

1.1. Preparation of aromatic diamine carbamate

Figure S1 shows the recovery rates and proportions of HBC and LBC co mponents from waste electrolyte.

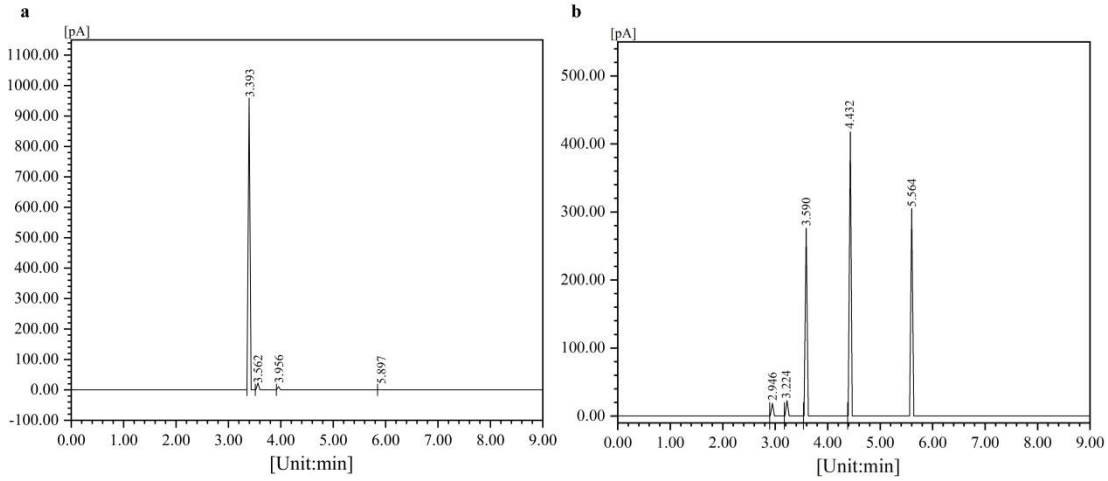

Figure S1. GC-MS curve

(a) HBC composition and proportion; (b) LBC composition and proportion.

Table S1. GC-MS Characterization Data of High/Low-Boiling Point Components in Waste Electrolyte

Product	GC-MS; Peak area (%)		
	Major components	Impurity	Retention time of Major components (min)
LBC	DMC: (27.615)	0.126	3.590
	EMC: (41.782)		4.432
	DEC: (30.477)		5.564
HBC	PC: (1.067)	0.471	3.393
	EC: (98.462)		3.562

1.2. Preparation of aromatic diamine carbamate

The main reagents included: 1,8-naphthediamine (97%), and 1,4-phenylenediamine (97%), LBC, 1,5,7-triazolane-4,4,0-diketide (TBD, 98%), 1,8-diazabicyclo[5.4.0]decane-5-en (DBU, 99%), and CH_3ONa (AR).

The reaction equation (Figure S2) and the experimental steps for synthesizing dicarbamate via the reaction of aromatic diamine with LBC are as follows

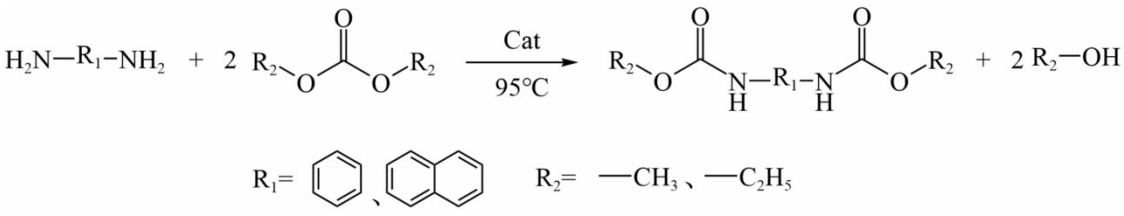

Figure S2 Principle of synthesis of dicarbamate

Two parallel experiments were conducted using LBC/1,8-naphthylendiamine (1,8-NDA) and LBC/1,4-phenylenediamine (1,4-PDA) as reaction systems at a molar ratio of 8:1. Corresponding reactants were added to a 250 mL three-neck flask, followed by a TBD-DBU-sodium methoxide (CH_3ONa) composite catalyst (molar ratio 2:2:1) representing 0.5% of the total reactant mass. Under nitrogen protection, the system was stirred under reflux condensation, continuously heated to boiling, and maintained for 6-8 hours. To prevent formation of azeotropic mixtures between alcohols and carbonates at reaction temperatures, a Soxhlet extractor containing molecular sieves was connected above the flask to adsorb these compounds, ensuring smooth reaction progression. As the reaction progressed, the precipitate gradually accumulated until stabilization, at which point the reaction was halted. The reaction mixture was filtered, with the residue washed three times with methanol. The combined filtrate and wash solution were centrifuged and concentrated to obtain precipitates. Collecting these precipitates along with the initial filter residue, the target products 1,8-naphthylendiamin

ecarboxylate (1,8-NPDC) and 1,4-phenylenediaminecarboxylate (1,4-BDC) were ultimately obtained.

1.3. Molecular dynamics simulation parameters

For the four blending systems (two pre-modified and two post-modified) in the synthesis process, the Forcite module was employed to configure force fields and perform charge calculations. The force field configuration utilized the cvff model, while the charge calculation employed the Change using QEq algorithm. For the four synthesized TPU molecular chains, the Forcite module was again used for force field configuration and charge calculation, with the cvff model selected. Due to the high atomic count, the Change using Gasteiger algorithm was adopted for charge calculation. Following these force field configurations and charge calculations, the Amorphous Cell module was applied to construct both the blending model and the polymer amorphous model.

The model employs the Smart (Steepest+ABNR+Quasi-Newton) optimization algorithm, with convergence criteria defined as Energy (kcal/mol) ≤ 0.001 and Force (kcal/mol Å) ≤ 0.5. Both the multiphase model of the pre-reaction mixture and the single-phase model of the post-reaction molecular chains utilize the NPT ensemble for equilibrium simulations and data collection. The NPT equilibrium was performed for 1000ps at 298K,0.0001GPa conditions, using the Nose-Hoover thermostat and Berendsen barostat. The simulation employed a time step of 1 fs, with a sampling frequency of 5000 and a total of 201 frames. Key parameters including the Root Mean Square Rotation Radius (Rg^2), Cohesion Energy Density (CED), and Hydrogen Bond Density were calculated from trajectory files and computational scripts.

1.4. Reagents and equipment.

PES prepolymer samples with different molecular weights were quantitatively dissolved in chloroform to prepare 1g/dL clear solutions. The solutions were heated in a water bath to 30°C and tested using a Ubelede viscometer. Both PES-chloroform solutions and pure chloroform were tested for drop time, with three independent

measurements per sample. The average drop time was calculated within the error range, using the equation parameters $K=2.4\times10^{-4}$, $\alpha=0.75$.

Table S2 Orthogonal experimental design for TPU modification

Number	Factor				f_{Perf}
	Diamine carbamate types	Diols types	Diol addition amount	PES formula weight	
1	1,8-NPDC	EG	10%	500	2.92
2	1,8-NPDC	BDO	15%	1000	1.68
3	1,8-NPDC	CHDM	20%	1500	0.59
4	1,8-NPDC	ISB	25%	2000	10.99
5	1,4-BDC	EG	15%	1500	11.97
6	1,4-BDC	BDO	10%	2000	1.27
7	1,4-BDC	CHDM	25%	500	0
8	1,4-BDC	ISB	20%	1000	0.42
9	1,8-NPDC	EG	20%	2000	0.16
10	1,8-NPDC	BDO	25%	1500	0
11	1,8-NPDC	CHDM	10%	1000	0.97
12	1,8-NPDC	ISB	15%	500	11.56
13	1,4-BDC	EG	25%	1000	1.24
14	1,4-BDC	BDO	20%	500	0.41
15	1,4-BDC	CHDM	15%	2000	0.76
16	1,4-BDC	ISB	10%	1500	12.32
K_{1j}	28.87	16.29	17.48	14.89	
K_{2j}	28.39	3.36	25.97	4.31	
K_{3j}	-	2.32	1.58	24.88	
K_{4j}	-	35.29	12.23	13.18	
K_{1i}	3.61	4.07	4.37	3.72	
K_{2i}	3.55	0.84	6.49	1.08	
K_{3i}	-	0.58	0.39	6.22	
K_{4i}	-	8.82	3.06	3.29	
R	0.12	7.42	5.49	4.63	

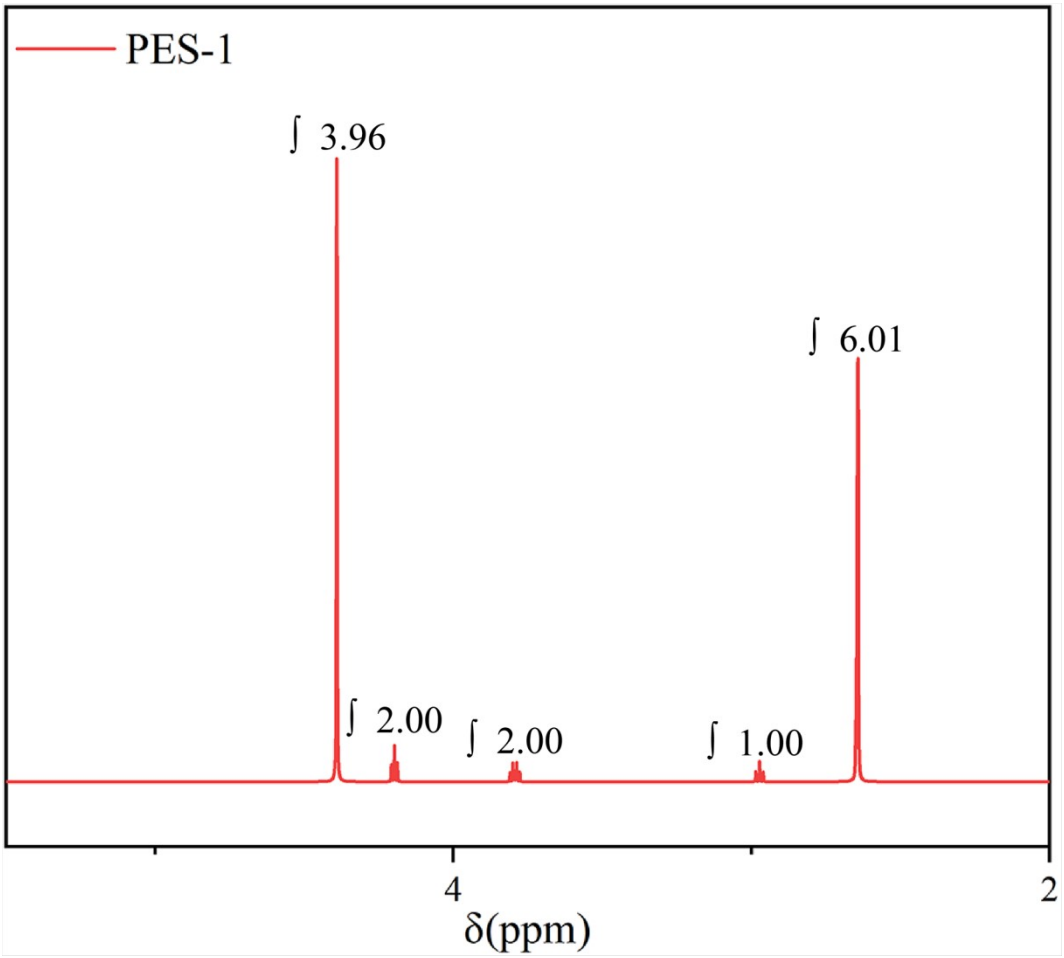

Figure S3 ^{1}H-NMR of PES-1

The ^{1}H NMR (500 MHz, chloroform) of PES-1 showed δ 4.39 (s, 8H), 4.20 (t, J = 4.9 Hz, 4H), 3.79 (dt, Ja = 6.5, Jb =5.0 Hz, 4H), 2.97 (t, J = 6.4 Hz, 2H), 2.64 (d, J = 1.5 Hz, 12H).

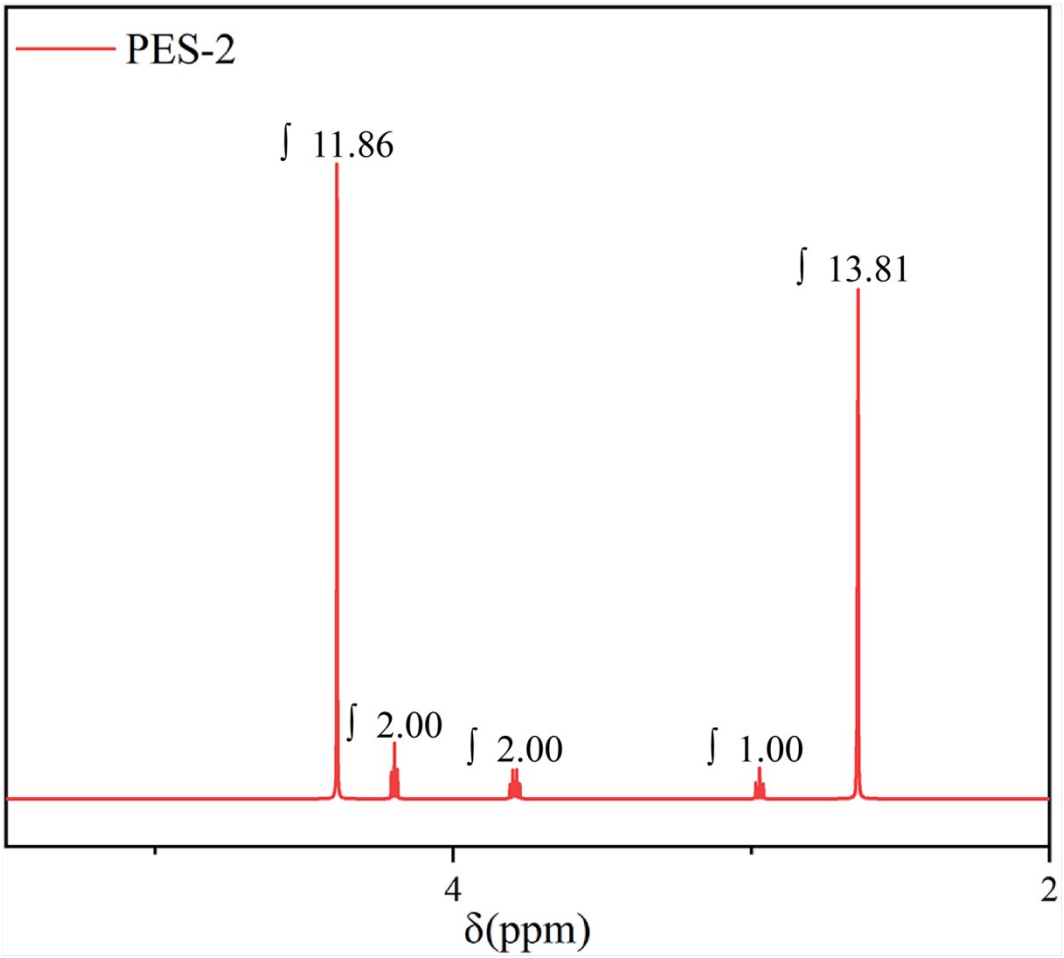

Figure S4 ^{1}H-NMR of PES-2

The ^{1}H NMR (500 MHz, chloroform) of PES-2 showed δ 4.39 (s, 24H), 4.20 (t, J = 4.9 Hz, 4H), 3.79 (dt, Ja = 6.5, Jb =5.0 Hz, 4H), 2.97 (t, J = 6.4 Hz, 2H), 2.64 (d, J = 1.1 Hz, 28H).

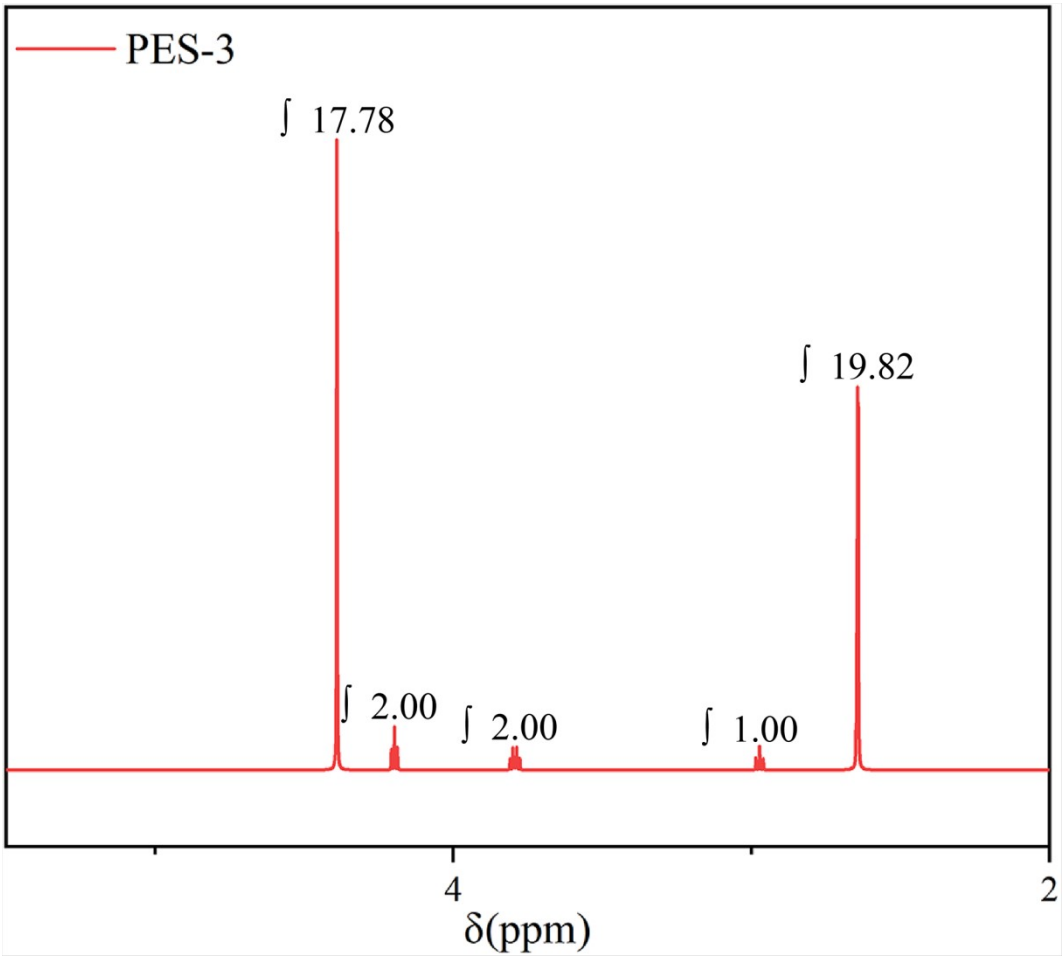

Figure S5 ^{1}H-NMR of PES-3

The ^{1}H NMR (500 MHz, chloroform) of PES-3 showed δ 4.39 (s, 36H), 4.20 (t, J = 4.9 Hz, 4H), 3.79 (dt, Ja = 6.5, Jb =5.0 Hz, 4H), 2.97 (t, J = 6.4 Hz, 2H), 2.64 (t, J = 1.2 Hz, 40H).

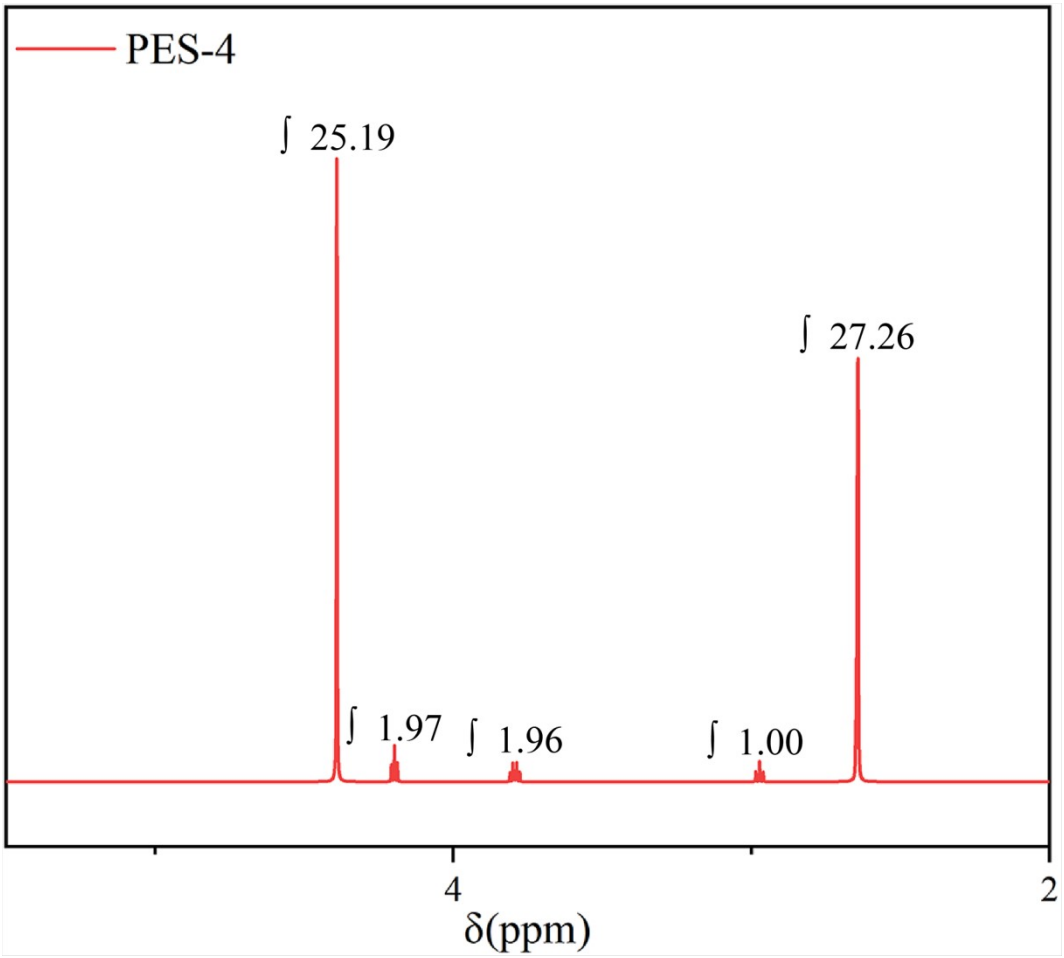

Figure S6 ^{1}H-NMR of PES-4

The ^{1}H NMR (500 MHz, chloroform) of PES-4 showed δ 4.39 (s, 52H), 4.20 (t, J = 4.9 Hz, 4H), 3.79 (dt, Ja = 6.5, Jb =5.0 Hz, 4H), 2.97 (t, J = 6.4 Hz, 2H), 2.64 (m, 56H).

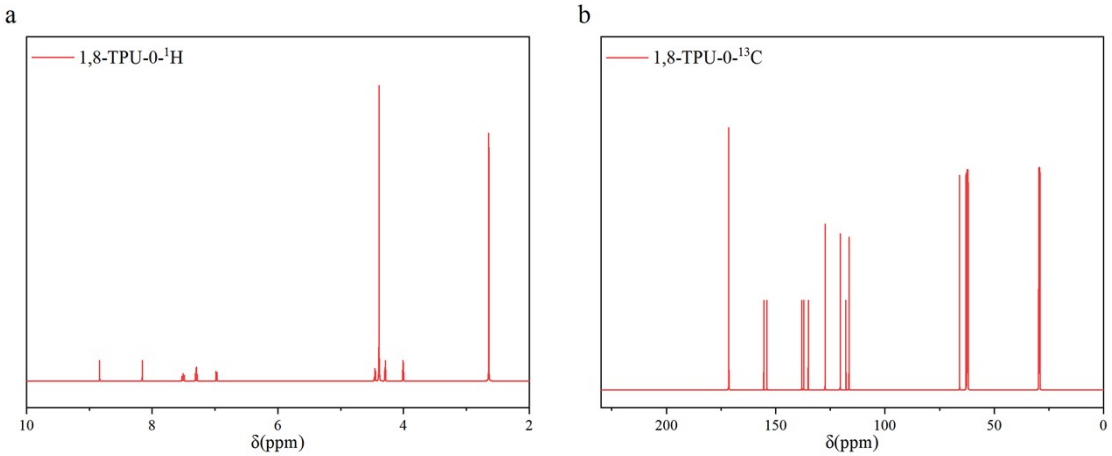

Figure S7 (a) ^{1}H-NMR of 1,8-TPU-0; (b) ^{13}C-NMR of 1,8-TPU-0

The ^{1}H NMR (500 MHz, chloroform) of 1,8-TPU-0 showed δ 8.84 (s, 1H), 8.16 (s, 1H), 7.51 (ddd, J = 9.3, 7.9, 1.0 Hz, 2H), 7.30 (t, J = 8.0 Hz, 2H), 6.98 (dt, J = 6.8, 1.0 Hz, 2H), 4.45 (m, 2H), 4.39 (s, 22H), 4.29 (t, J = 4.2 Hz, 2H), 4.01 (t, J = 4.2 Hz, 2H), 2.64 (d, J = 0.9 Hz, 24H).^{13}C NMR (125 MHz, Chloroform) δ 175.66, 159.19, 146.81, 140.69, 134.50, 128.78, 122.82, 117.87, 108.37, 63.28, 28.62.

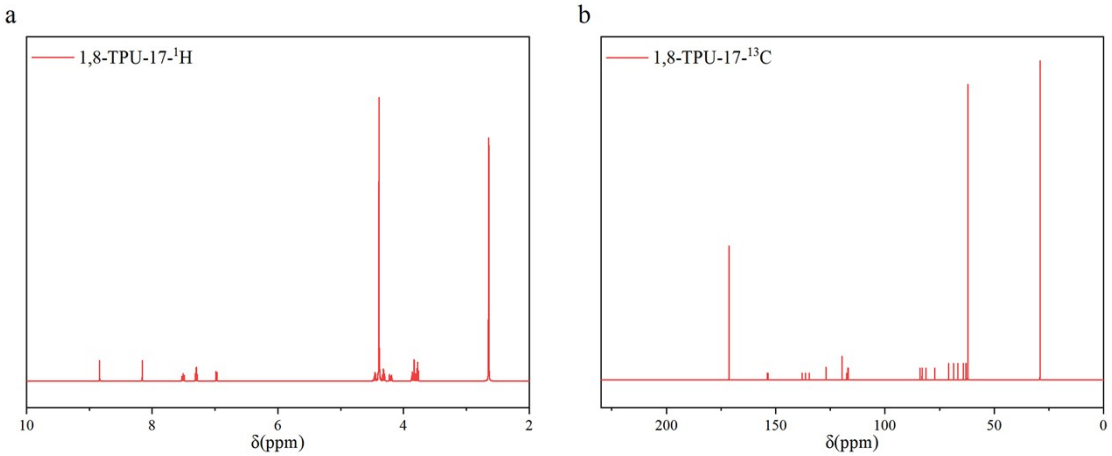

Figure S8 (a) ^{1}H-NMR of 1,8-TPU-17; (b) ^{13}C-NMR of 1,8-TPU-17

The ^{1}H NMR (500 MHz, chloroform) of 1,8-TPU-17 showed δ 8.84 (s, 1H), 8.16 (s, 1H), 7.51 (ddd, J = 9.3, 7.9, 1.0 Hz, 3H), 7.30 (t, J = 8.0 Hz, 3H), 6.98 (dt, J = 6.7, 1.0 Hz, 3H), 4.46 (td, J = 5.1, 3.2 Hz, 3H), 4.39 (d, J = 1.1 Hz, 54H), 4.31 (m, 4H), 4.20 (m, 2H), 3.86 (m, 2H), 3.83 (d, J = 2.4 Hz, 2H), 3.81 (d, J = 3.1 Hz, 2H), 3.78 (t, J = 5.7 Hz, 2H), 2.64 (m, 54H).^{13}C NMR (125 MHz, Chloroform) δ 171.32, 153.62, 136.30, 126.93, 119.61, 116.88, 116.76, 84.00, 83.07, 81.22, 70.96, 68.56, 66.66, 64.25, 62.93, 62.07, 29.07.

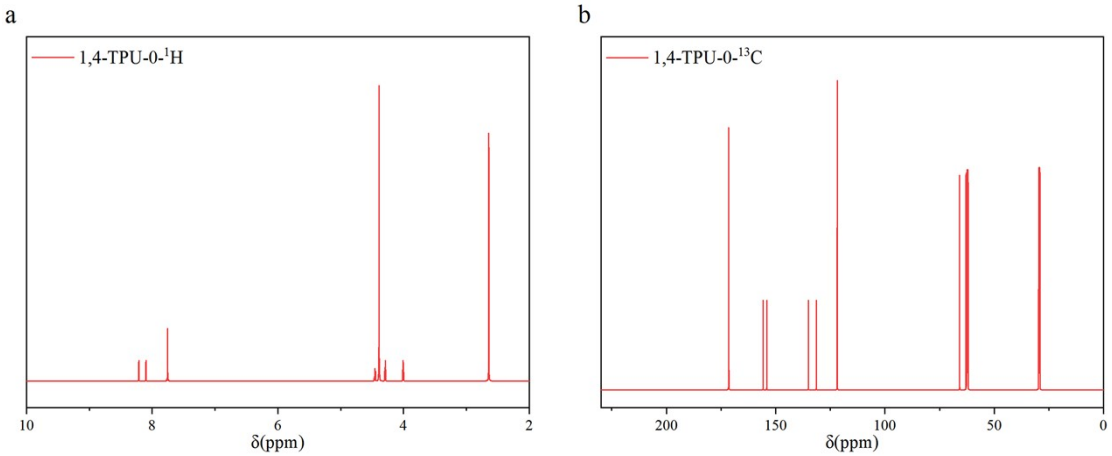

Figure S9 (a) ^{1}H-NMR of 1,4-TPU-0; (b) ^{13}C-NMR of 1,4-TPU-0

The ^{1}H NMR (500 MHz, chloroform) of 1,4-TPU-0 showed δ 8.21 (s, 1H), 8.10 (s, 1H), 7.75 (s, 5H), 4.45 (m, 3H), 4.39 (s, 29H), 4.29 (t, J = 4.2 Hz, 3H), 4.01 (t, J = 4.2 Hz, 3H), 2.64 (d, J = 0.9 Hz, 31H).13C NMR (125 MHz, Chloroform) δ 177.84, 162.77, 158.88, 149.10, 128.15, 121.11, 113.90, 63.24, 28.70.

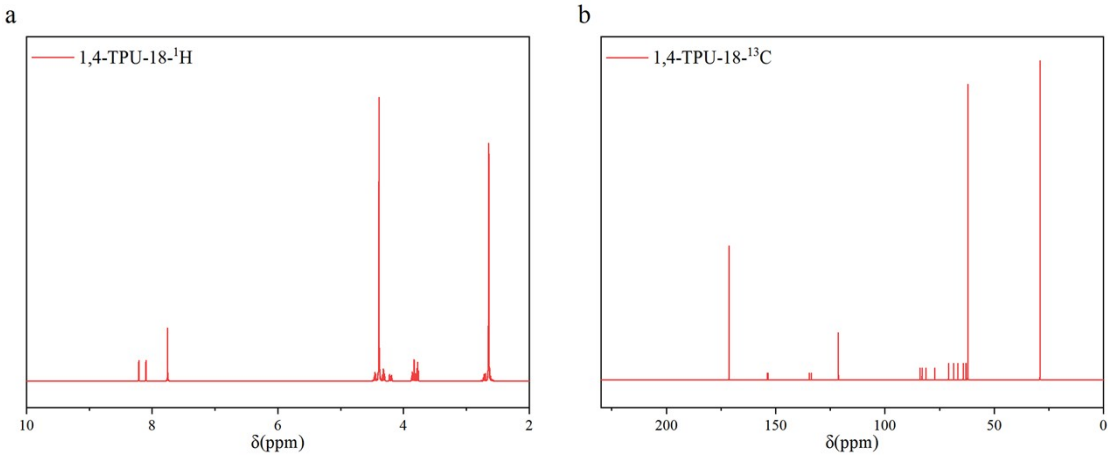

Figure S10 (a) ^{1}H-NMR of 1,4-TPU-18; (b) ^{13}C-NMR of 1,4-TPU-18

The ^{1}H NMR (500 MHz, chloroform) of 1,4-TPU-18 showed δ 8.21 (s, 1H), 8.10 (s, 1H), 7.75 (s, 5H), 4.45 (m, 3H), 4.39 (d, J = 1.1 Hz, 54H), 4.31 (m, 4H), 4.20 (m, 2H), 3.82 (m, 8H), 2.71 (m, 2H), 2.65 (m, 53H).13C NMR (125 MHz, Chloroform) δ 171.32, 153.61, 134.11, 121.31, 84.01, 83.07, 81.22, 77.27, 70.96, 68.56, 66.66, 64 25, 62.92, 62.07, 29.06.

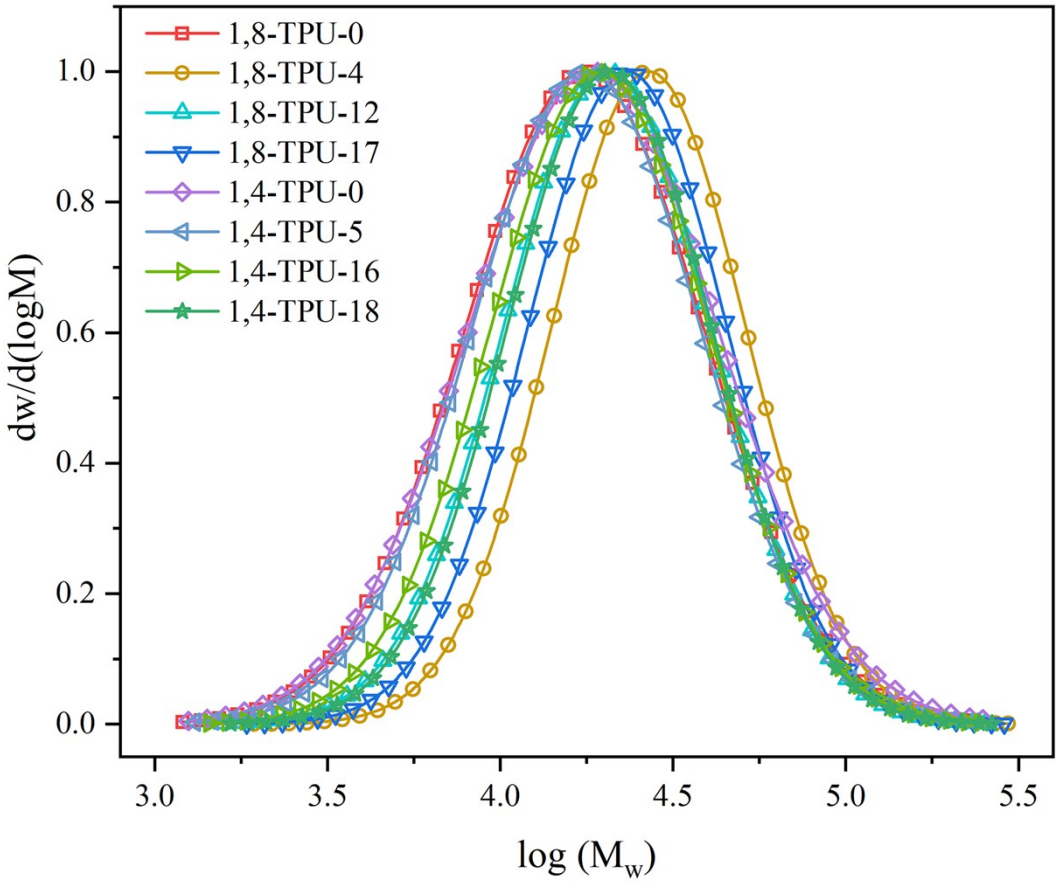

Figure S11 GPC curve of TPU